2015

Synthesis, Linear and Nonlinear Photophysical Characterization of Two Symmetrical Pyrene-terminated Squaraine Derivatives in Solution

Alfonso Ballestas Barrientos
University of Central Florida

SYNTHESIS, LINEAR AND NONLINEAR PHOTOPHYSICAL CHARACTERIZATION OF TWO SYMMETRICAL PYRENE-TERMINATED SQUARAINE DERIVATIVES IN SOLUTION

by

ALFONSO RAFAEL BALLESTAS BARRIENTOS
B.S. Universidad del Zulia, 2011

A thesis submitted in partial fulfillment of the requirements
for the degree of Master of Science
in the Department of Chemistry
in the College of Sciences
at the University of Central Florida
Orlando, Florida

Spring Term
2015

Major Professor: Kevin D. Belfield

ABSTRACT

Two indole-based squaraine dyes bonded to two pyrenyl groups through vinyl- and ethynyl- linkers were synthesized with the aim of enhancing the intramolecular charge transfer interaction in addition to improving their optical properties. The absorption and emission properties of these derivatives were determined in order to gain an insight into the intensity of this type of interaction, their aggregation behavior and compare them with results obtained through quantum chemical calculations. Both compounds presented high photochemical stability in THF, and the linear spectroscopic characterization revealed high extinction coefficients, large fluorescence quantum yields and relatively low tendency of forming excimers in several solvents. The nonlinear spectroscopic study revealed two-photon absorption cross section maxima greater than 10,000 GM (1 GM = 1×10^{-50} cm^4 s/photon), which are improved values in comparison with the indole-based squaraine core. The experimental results were compared with time-dependent DFT calculations. These observations propose a new trend in the formulation of highly absorbing organic molecules containing pyrenyl groups for the development of new materials with Organic Light-Emitting Diode (OLED) applications. Moreover, this work contributes to the study of intramolecular charge transfer interaction and its tailoring for the improvement of the linear and nonlinear optical properties.

To my family, friends, and everyone who has supported and inspired me over the past 27 years

ACKNOWLEDGMENT

This has been one of the biggest adventures of all times and it is the perfect time to thanks God, my family, friends and professors that has stood with me during the past 2 years. I would also like to thanks Dr Belfield and his research group for their support, expertise and guidance. Thanks to the Chemistry department for assisting me while doing the Master Program. Finally, I would like to thanks the Venezuela-U.S. Fulbright Program for a Master Fellowship and for giving me the opportunity of being part of such a recognize and talented organization.

TABLE OF CONTENTS

LIST OF FIGURES

LIST OF TABLES

CHAPTER 1: INTRODUCTION

Based on the pioneering studies of organic light-emitting diodes (OLEDs)[1] an effort has been made to synthesize and characterize organic compounds with linear and nonlinear optical (NLO) properties that are adequate for optoelectronic devices.[1-5] Among these compounds, those containing polycyclic aromatic hydrocarbons (PAHs) have drawn much attention due to their extended π-conjugation that provides them with unique photophysical and charge transport properties.[6-7]

Pyrene belongs to the family of the PAHs, and its use in the design of optical devices has increased due to its tunable electrochemical and photophysical properties as a result of its strong π-electron delocalization over the four fused benzene rings, the possibility of suitable substitution at different positions, and good thermal stability.[6, 8] Pyrene derivatives have been used in electronic devices, such as OLED's, organic field-effect transistors (OFETs)[9-11] and organic photovoltaic devices (OPVs).[3] In the same way, their application in the synthesis of hydrophobically labeled water soluble polymers, in the labeling of oligonucleotides for DNA assay,[12] and as a microenviroment probe have been previously reported.[13] On the other hand, while the concentration effect in the quenching of the molecular fluorescence of pyrene derivatives limits their application in optoelectronic devices,[14-17] the appearance of the excimer emission signal can be beneficial for the design of fluorescence sensors of solvent polarity or viscosity and for the targeting of specific sequences in DNA.[18]

The application of the two-photon absorption (2PA) process in numerous fields, including optical data storage storage,[19] photodynamic therapy (PDT),[20] fluorescence bioimaging,[21] three-dimensional (3D) microfabrication,[22] and upconverted lasing,[23] has encouraged the search for new

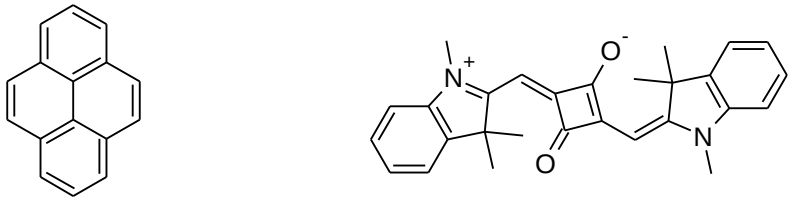

(a) (b)

Figure 1. Molecular Structure of pyrene (a) and an indole-based squaraine dye (b)

organic dyes based on the squaraine core (C_4O_2). Squaraine dyes are very attractive polymethine-like structures owing to their strong electron withdrawing character, and when attached to electron donor groups can exhibit intramolecular charge transfer as well as two-photon absorption properties.[24-27] Both their intense absorption in the visible-NIR spectral range and their associated emission arise from their donor-acceptor-donor (D-A-D) charge transfer interaction, which provides these organic dyes with a high transition dipole moment and a resonance stabilization of the zwitterionic structure.[28-35] In order to exploit the advantages of these derivatives, the nature of the donor groups in 1,3-disubstitued squaraine dyes has been tailored to enhance their 2PA, typically by trying to increase their donor character while extending the π-conjugation of the molecular system. The synthetic strategies, potential applications, and structure-property relations of these types of squaraine dyes have been extensively studied.[24-27, 31, 34-38]

In our previous work[39] two squaraine units were attached to a central fluorene core via ethyne bridges. Ethyne bridges were chosen to enhance planarity and therefore the conjugation between the squaraine groups and fluorene.[40-41] Quantum calculations on the two photon absorption behavior of this molecule indicated that the highest 2PA cross sections were due to intramolecular charge transfer between the fluorene and the two squaraines. This conclusion is in agreement with the accepted understanding that high two photon absorption is related to the degree

of intramolecular charge transfer.[42] It is therefore likely that the functionalization of a squaraine core with pyrenyl groups would lead to the enhancement of the electronic transfer interaction which may also result in a greater 2PA cross-section desirable for biological and optoelectronic applications.[43] Herein, we have synthesized two pyrene terminated 1,3-disubstitued indole-based squaraine dyes using vinyl and ethynyl linkages and studied their linear and NLO properties in solution. With the implementation of these two linkers we expected to favor the coplanarity of the system in order to enhance the electron charge transfer interaction through the whole π-conjugated system.[44-46]

With the aim of examining the photophysical properties of these two pyrenyl-terminated squaraine dyes, we synthesized both the vinyl and ethynyl linked dyes and conducted the following measurements on each one: (1) one-photon absorption, photochemical stability, fluorescence emission and quantum yield in dichloromethane (DCM), tetrahydrofuran (THF) and toluene (TOL); (2) excitation anisotropy; (3) spectral changes induced by the presence of water; (4) concentration dependence of the fluorescence emission; and (5) 2PA of both dyes. In addition quantum chemical calculations were performed in order to better understand and interpret experimental results.

CHAPTER 2: MATERIALS AND METHODS

2.1 Experimental details

All reagents and solvents were used as received from commercial suppliers unless otherwise noted. ^{1}H and ^{13}C NMR spectra were acquired on a Varian NMR spectrometer at 500 and 125 MHz, respectively. High resolution MS was performed at the University of Florida. 1-Ethynylpyrene was purchased from VWR International. The synthesis of both 1 and 2 are shown in Scheme 1. Preparation of 4 and 5 were done following the procedure reported in our previous work[39]. 1-vinylpyrene was synthesized according to the method proposed in the literature[47].

2.2 Preparation of 2,4-Bis[(5-Bromo-1-ethyl-3,3-dimethyl-2,3- dihydroindol-2-ylidene)methyl] cyclobutenediylium-1,3-diolate (7).

5-Bromo-1-ethyl-2, 3, 3-trimethyl-3H-indolium iodide (0.610 g, 1.55 mmol) was suspended in hexane (6 mL) under nitrogen. Aqueous sodium hydroxide (4 N) was added (0.6 mL) with vigorous stirring, and the solution slowly turned clear yellow as the solid dissolved. The aqueous layer was removed and the organic layer was washed two times with deionized water. This hexane solution of methylene base was then added to a suspension of squaric acid (0.086 g, 0.75 mmol) in a mixture of toluene (15 mL) and 1-butanol (15 mL). The mixture was then refluxed using a Dean-Stark trap for a total of three hours. The color turned slowly to dark blue once the temperature increased to over 100°C. The reaction was then cooled to room temperature, solvent was removed under vacuum, and the resulting solid was dissolved in CH_2Cl_2 and purified by column chromatography (beginning with pure CH_2Cl_2 and increasing to 2% methanol in CH_2Cl_2) to yield 411 mg (89%) of a copper-colored crystalline solid. Final purification was accomplished by recrystallization in dichloromethane/cyclohexane. ^{1}H NMR (500 MHz, $CDCl_3$) δ 1.28 – 1.49

(6 H, t, *J* 7.2), 1.68 – 1.89 (12 H, s), 3.91 – 4.19 (4 H, broad s), 5.89 – 6.03 (2 H, s), 6.84 – 6.88 (2 H, d, *J* 8.3), 7.41 – 7.45 (2 H, dd, *J* 8.3, 1.9), 7.45 – 7.49 (1 H, d, *J* 1.8). ^{13}C NMR (126 MHz, $CDCl_3$) δ 11.92, 27.00, 38.56, 49.40, 86.78, 110.41, 116.64, 125.79, 130.73, 141.02, 144.46, 169.10, 180.57, 182.13. Anal. Calcd. for $C_{30}H_{30}N_2O_2Br_2$: C, 59.04; H, 4.92; N, 4.59; found C, 58.86; H, 5.03; N, 4.58.

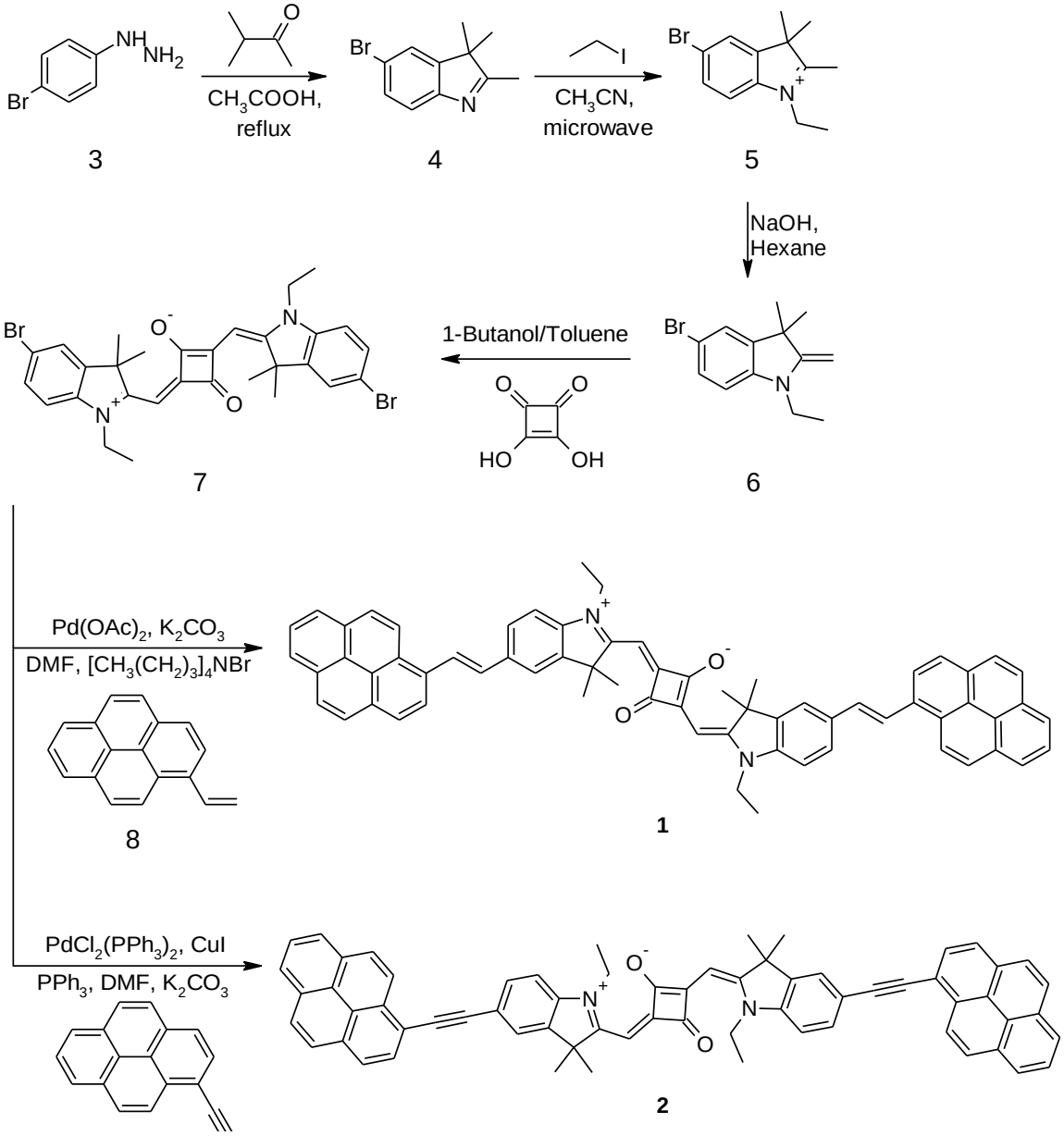

Scheme 1: Synthesis of 1 and 2

2.3 Preparation of 2,4-Bis[(5-{1-vinylpyrene}-1-ethyl-3,3-dimethyl-2,3-dihydroindol-2-ylidene)methyl]cyclobutenediylium-1,3-diiolate (1).

2,4-Bis[(5-Bromo-1-ethyl-3,3-dimethyl-2,3-dihydroindol-2-ylidene)methyl] cyclobutenediylium-1,3-diolate (0.334 g, 0.55 mmol), Palladium(II) acetate (0.004 g, 0.02 mmol), cesium carbonate (0.448 g, 1.38 mmol) and Tetra-n-butylammonium bromide (0.354 g, 1.09 mmol) and N,N-Dimethylformamide (10 ml) were mixed in N_2 atmosphere. Then 1-vinylpyrene 0.250 g, 1.09 mmol) was added and the mixture was heated to 80 °C. The reaction was followed by TLC. After 80 h the reaction was cooled and solvent was removed under vacuum. The resulting solid was purified by an Isolera flash chromatography system using CH_2Cl_2 and increasing to 1% methanol in CH2Cl2 to yield 0.345 g, (69 %) of green solid. ^{1}H NMR (500 MHz, $CDCl_3$) δ 1.46 (6 H, t, *J* = 7.21 Hz), 1.91 (12 H, s), 4.14 (4 H, s), 6.04 (2 H, s), 7.06 (2 H, d, *J* = 8.07 Hz), 7.38 (1 H, s), 7.42 (1 H, s), 7.62 (2 H, dd, *J* = 8.19, 1.59 Hz), 7.72 (2H, d, *J* = 1.47 Hz), 8.00 - 8.22 (16 H, m), 8.34 (2 H, d, *J* = 7.83 Hz), 8.55 (2 H, d, *J* = 9.54 Hz). ^{13}C NMR (126 MHz, $CDCl_3$) δ 12.16, 27.19, 38.64, 49.3, 86.95, 109.38, 120.16, 123.07, 123.59, 124.81, 125.01, 125.08, 125.19, 125.33, 126.05, 127.2, 127.3, 127.48, 127.65, 128.38, 130.86, 131, 131.33, 131.58, 131.96, 133.94, 134.2, 141.79, 143.13, 169.21, 179.54, 182.44. HR-MS theoretical m/z $[M+H]^+$ = 905.4101; found $[M+H]^+$ = 905.4054.

2.4 Preparation of 2,4-Bis[(5-{1-ethynylpyrene}-1-ethyl-3,3-dimethyl-2,3-dihydroindol-2-ylidene)methyl]cyclobutenediylium-1,3-diiolate (2).

2,4-Bis[(5-Bromo-1-ethyl-3,3-dimethyl-2,3-dihydroindol-2-ylidene)methyl] cyclobutenediylium-1,3-diolate (10) (0.305 g, 0.50 mmol), dichlorobis(benzonitrile)palladium(II) (0.015 g, 0.04 mmol), copper(I) iodide (0.008 g, 0.04 mmol), triphenylphosphine (0.017 g, 0.06 mmol), diisopropylamine (0.6 mL) and toluene (14 mL) were all combined in a sealed reaction

tube in a glovebox. 1-ethynylpyrene (0.232 g, 1.03 mmol) was added and the mixture was heated to 60 - 65°C. The reaction was followed by TLC. After 80 h the reaction was cooled and solvent was removed under vacuum. The resulting green solid was purified by column chromatography beginning with pure CH_2Cl_2 and increasing to 1% methanol in CH_2Cl_2 to yield 0.076 g (17%) of green solid. Final purification was accomplished by recrystallization in dichloromethane/methanol. ^{1}H NMR δ_H (500 MHz, CD_2Cl_2) 1.38 – 1.53 (6 H, t, *J* 7.3), 1.83 – 1.98 (12 H, s), 4.08 – 4.26 (4 H, s), 5.99 – 6.12 (2 H, s), 7.07 – 7.20 (2 H, d, *J* 8.7), 7.68 – 7.83 (4 H, m), 8.05 – 8.36 (16 H, m), 8.69 – 8.80 (2 H, d, *J* 9.1). ^{13}C NMR (126 MHz, CD_2Cl_2) δ 12.33, 27.25, 39.13, 49.60, 87.65, 89.06, 95.96, 109.85, 118.26, 118.76, 124.69, 124.89, 125.07, 125.85, 125.96, 126.08, 126.80, 127.65, 128.57, 128.81, 129.92, 131.53, 131.66, 131.73, 132.12, 132.27, 142.70, 143.08, 169.54, 181.47, 182.03. HR-MS theoretical m/z $[M-H]^+$ = 899.3632 and $[M+CH_3]^+$ = 915.3945; found $[M-H]^+$ = 899.3640 and $[M+CH_3]^+$ = 915.3912.

2.5 Linear Characterizations.

Absorption measurements were performed on an Agilent 8453, and fluorescence measurements on an Edinburgh Instruments FLS980. Solutions of the compounds (~ 10^{-6} M) were prepared in 10 mm quartz cuvettes using spectroscopic grade solvents. Fluorescence spectra were collected using a red-sensitive photomultiplier (PMT), and corrected for the responsivity of the detector. Quantum yields of fluorescence were calculated relative to a standard: Cresyl violet (Φ_f = 0.54).[48] Excitation anisotropy measurements were performed in the viscous solvent silicone oil so as to retard the molecular rotational movements. Lifetime decays of the observed fluorescence signals were determined using a 670 nm EPL diode laser, with a time resolution of ≈ 0.2 ns.

Photodecomposition quantum yields, Φ_{Ph}, were determined through irradiating sample solutions with a 650 nm diode laser (≈ 500 mW cm^{-2}) and recording absorption spectra at timed intervals. This data was used in equation (1), where D(λ, 0), D(λ, t_{ir}), ε(λ), t and λ are the initial and final optical density of the solution, extinction coefficient (M^{-1} cm^{-1}), irradiation time (s) and excitation wavelength, respectively; N_A the Avogadro's number; t_{ir} the total irradiation time; $I_0(\lambda)$ is the spectral distribution of the excitation irradiance.[30]

$$\Phi_{Ph} = \frac{[D(\lambda,0) - D(\lambda,t_{ir})]N_A}{10^3 \cdot \varepsilon(\lambda) \cdot \int_\lambda \int_0^{t_{ir}} I_0(\lambda)\,[1 - 10^{-D(\lambda,t)}]d\lambda\, dt} \quad (1)$$

2.6 Non-Linear Photophysical Characterizations

Degenerate two-photon absorption measurements were collected over a broad spectral region through the open aperture Z-scan technique utilising an amplified femtosecond laser system (Coherent Inc.).[29] Solutions of the compounds were prepared in DCM in the range 10^{-2} to 10^{-4} M. The 800 nm output of a Mira 900-F Ti:sapphire laser (repetition rate, f = 76 MHz; average power ≈ 1.1 W; pulse duration, τP ≈ 200 fs) pumped by the second harmonic of CW Nd^{3+}:YAG laser (Verdi-10), was regeneratively amplified with a 1 kHz repetition rate (Legend Elite USP) providing ≈ 100 fs pulses (FWHM) with energy ≈ 3.6 mJ $pulse^{-1}$. This output at 800 nm was used to pump an ultrafast optical parametric amplifier (OPerA Solo (OPA), Coherent Inc.) with a tuning range 0.24–20 μm, τP ≈ 100 fs (FWHM), and pulse energies, EP, up to ≈100 mJ. This setup is described in previous literature.[28]

2.7 Quantum Chemical Calculations

Density functional theory (DFT) calculations were performed on the molecules with the GAUSSIAN09 software package.[49] The structures were initially optimized using the B3LYP DFT

method, with D95* basis set. Using these optimized structures, time dependent DFT (TD-DFT) calculations were run using the same B3LYP method. Interactions of solvent were not incorporated into the calculations. Visualization of the structures and molecular orbitals was acheived through Jmol.

CHAPTER 3: RESULTS AND DISCUSSION

3.1 Synthesis of pyrene-terminated squaraine dyes

The synthesis of both 1 and 2 are shown in Scheme 1 (p. 5). Preparation of 1-vinylperene was done via Witting reaction following a previously reported procedure.[47] In both cases, the indole derivative (4) was first synthesized via Fisher condensation and then alkylated using microwave radiation to produce compound 5 with high yield. Subsequently, the symmetrical bromo-substituted indole based squaraine dye (7) was obtained by the condensation of squaric acid with the methylene base (6) in a toluene/n-butanol mixture under azeotropic distillation conditions.[39] Finally, compound 7 was used to synthesize 1 via Heck coupling with 1-vinylpyrene and 2 via Sonogashira coupling with 1-ethynylpyrene.

3.2 Photophysical Characterizations

The absorption spectra for the two compounds show the characteristic sharp peak for a squaraine based dye at ca. 680 nm (Figure 1),[24, 39] with additional bands seen below 450 nm attributable to the pyrene moieties that terminate the molecules. The anticipated vibrational shoulder at 641 nm appears enveloped by the main absorption for 1, though it remains visible for 2 (at 630 nm). Despite this, the emission spectra for both compounds feature this shoulder, creating an approximate mirror image.[48] In both cases, the compounds exhibit a very small Stokes shift (Table 1), typical for molecules of this type, since the geometry of the excited state is not dissimilar from that of the ground state.[39]

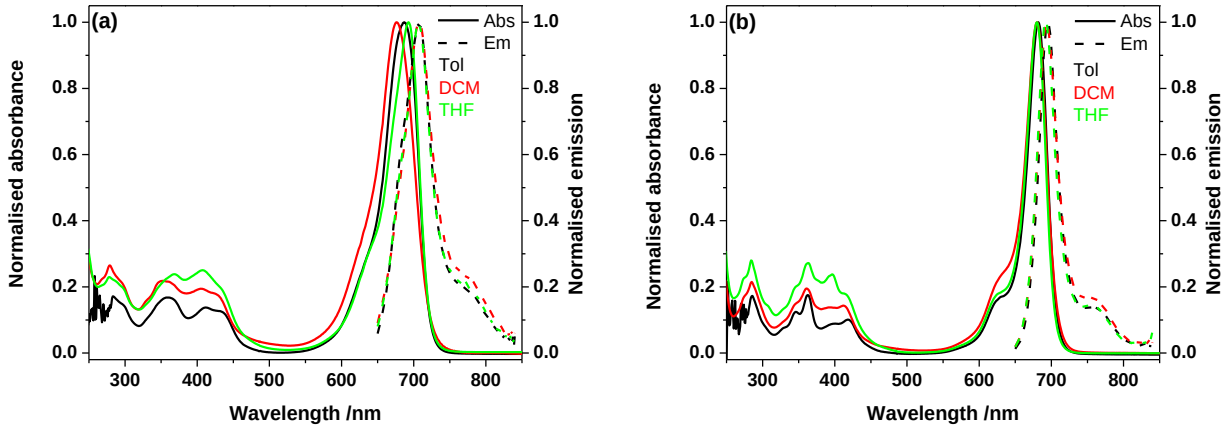

Figure 2: Absorption (solid lines) and emission (dashed lines) spectra of 1 (a) and 2 (b) in TOL (black), DCM (red) and THF (green).

Table 1: Linear photophysical data for 1 and 2

	1			2		
	TOL	DCM	THF	TOL	DCM	THF
λ_{max}^{abs} [a] /nm	687	676	693	682	680	680
ε[b] /10^3 M^{-1} cm^{-1}	199	190	199	241	328	287
λ_{max}^{em} [a] /nm	707	709	706	695	694	692
$\Delta\lambda$[c] /cm^{-1}	412	689	266	274	297	255
ϕ_f[d]	0.68	0.46	0.6	0.79	0.66	0.72
τ[e] /ns	2.1	1.5	1.8	2.1	1.9	2
ϕ_{Ph} /10^{-6}			19.3			23.6

[a] Absorption and emission maxima ±1 nm; [b] extinction coefficients ±5%; [c] Stokes shift ±2 nm; [d] fluorescence quantum yields ±10%; [e] fluorescence lifetimes ±10%.

The peak of the main absorption band of 1 shows mild fluctuation with solvent polarity (676-693 nm), though its emission maxima show more consistency (706-709 nm); meanwhile 2 retains constancy for both absorption (680-682 nm) and emission (692-695 nm) maxima. The small increase in Stokes shift for 1 with the vinylene linker compared to 2 having the ethynylene linker is consistent with other reports on the effects of these linkers.[50] The extinction coefficients,

ε, for both compounds are very high across the investigated solvents, similar to previously reported squaraine compounds.[24, 39]

The increased fluorescence quantum yields for 2 compared to 1 can be explained by the increased rigidity provided by the triple bond linkers, whereas the double bond still allows a limited amount of rotation that would expend energy prior to emission. Despite the consistency of these efficiencies for 2, there is an anomaly in the case of 1: a lower quantum yield in DCM was obtained, though this coincides with a shorter lifetime of the fluorescence.

Excitation anisotropy traces recorded for the two compounds (Figure 2) exhibit a noted similarity to one another, albeit with 1 displaying a greater lean towards an orthogonal emission at ca. 450 nm than 2. The plateau running from ca. 530 nm to 660 nm indicates that excitation in this region will result in achieving the same electronically excited state.

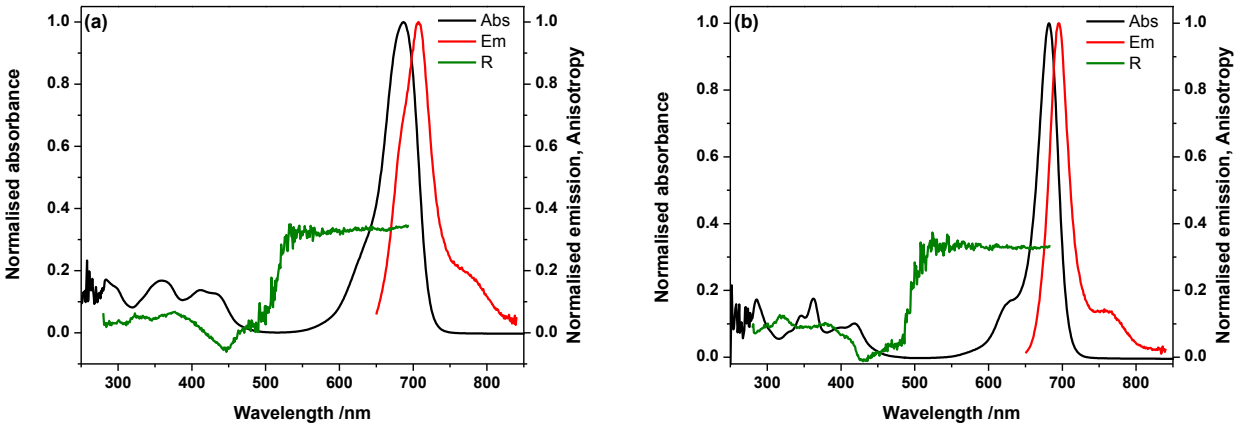

Figure 3: Excitation anisotropy traces (dark green) for 1 (a) and 2 (b) overlaid on the respective absorption (black) and emission (red) spectra in TOL.

In this work, the photochemical decomposition quantum yields for 1 and 2 were determined in THF. This parameter comes to relevance in photonic as well as in photobiological applications and it is independent of excitation settings during the experiment.[24, 29] Both dyes synthesized in

this study showed an improved photochemical stability in THF by 2 orders of magnitude compared with previously reported coumarin dyes,[51-53] which are considered in the literature as highly photostable compounds with potential optoelectronic applications. The difference in the photostability among the two dyes synthesized in this work can be explained on the basis of the nature of the linkers used and the intramolecular interactions. Dye 2 showed a higher photostability since the ethynyl bridge provides a stronger bond and a greater rigidity to the system. In the same way, this linker also permits a higher conjugation in the π-system compared to dye 1 in which the vinylene bridge allows the structure to twist out of the conjugation due to steric interaction.[54] This assumption is also borne out by quantum chemical calculations further shown below.

Investigation of the two-photon absorbing properties of the two compounds (Figure 3) in both cases revealed maxima exceeding 10,000 GM, not uncommon for squaraine based dyes, due to the combination of large transition dipole between the ground and excited state, and the small detuning energy once the excited state is reached.[24] The peak of this band could not be resolved however, due to the overlap with the one-photon absorption band. It is noted, though, that both compounds possess a 'plateau' of near-constant cross section at ca. 820-1020 nm, and 840-960 nm, respectively. The maximum 2PA cross section was measured to be slightly higher for the ethynylene linked compound, but the plateau of near-constant cross section extends over a larger wavelength range for the vinylene linker (200 nm vs 120 nm). These relatively small differences are in keeping with reports in the literature that the effect of the type of linker is not usually large.[50, 54]

A second band emerges around 1300 nm, overlapping with the vibrational shoulder of the linear absorption. Formally, this transition is forbidden due to the symmetry of the molecules, though the selection rules are bent to accommodate the asymmetrical vibrations.[24]

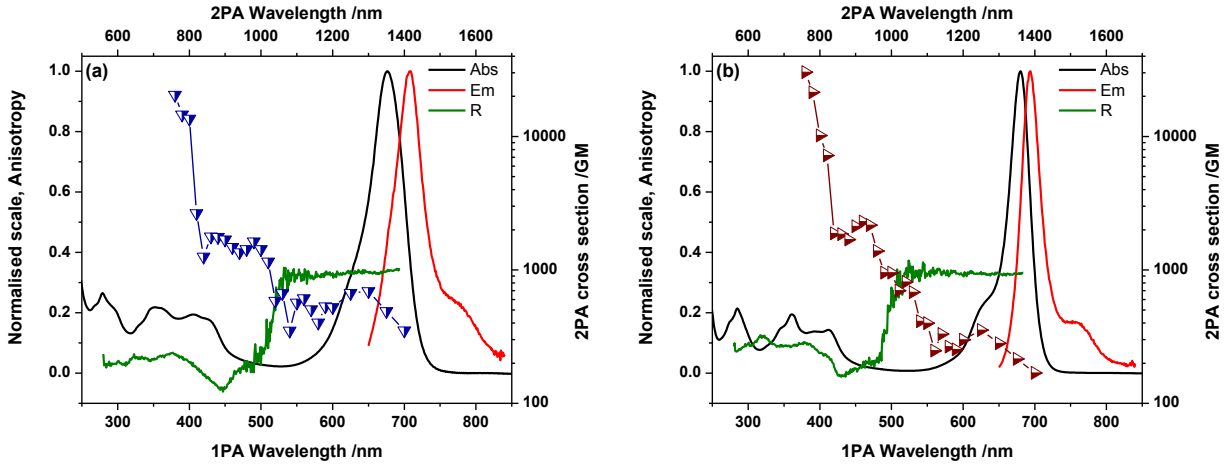

Figure 4: Two-photon absorption spectra for 1 (a, dark blue) and 2 (b, dark red) in DCM overlaid on the respective one-photon absorption (black) and emission (red) spectra in DCM and excitation anisotropy traces (dark green).

3.3 Water-induced aggregation of dyes in THF

It is evident from the molecular structure that the addition of pyrenyl moieties to the squaraine core would enhance the aggregation properties due to intermolecular interaction.[6, 55-56] In order to gain some insight about this process, the absorption spectra of both 1 and 2 were recorded in several THF-water mixtures at constant dye concentrations of 6×10^{-6} mol/L and 3.5×10^{-6} mol/L respectively (Figure 4).

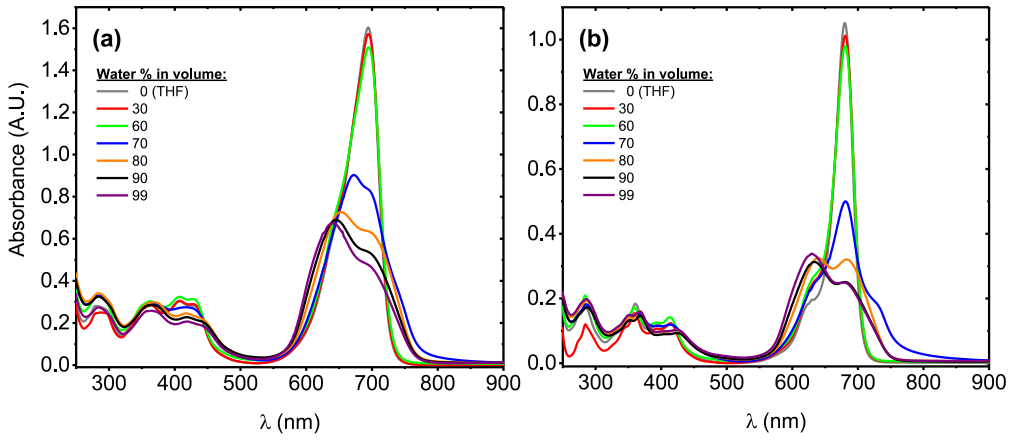

Figure 5: Absorption spectra of 1 (a) and 2 (b) as a function of water percentage in THF-water binary mixtures.

The spectra revealed a new blue-shifted band appearing at 641 and 630 nm for the 1 and 2 respectively with a bandwidth of the same order of the monomer band. This spectral behavior indicates the formation of H-aggregates in solution and it becomes relevant once the water composition reaches levels higher than 60 % in volume. This can be explained on the bases of the water-THF hydrogen bond formation, at low water concentration levels the solvent-solvent interaction becomes relevant and the dye-water interaction is negligible, however as the water content in the medium becomes larger, the hydrophobic interaction induces the dye molecules to form aggregates to exclude water molecules and reduce the surface tension. As the exciton model describes for associated molecules,[57] a decrease in the fluorescence quantum yield is expected to occur due to a relaxation from the H-band to a forbidden lower energy level.[55-56, 58-59] It is also known that pyrene derivatives are able to form aggregates in the excited state (excimers) due to intermolecular interactions. This observation lead us to develop a concentration dependence study of both dyes in different solvents.

3.4 Excimer study of dyes

The emission spectra of both dyes in solution were measured in different solvents and their concentration dependence is plotted in Figure 5. For all the solvents used, a shift towards longer wavelength occurred as the concentration of the dyes increased, which is usual for compounds with small Stokes shift and is the result of the reabsorption of the short wavelength region of the fluorescence that is emitted by the sample.[48]

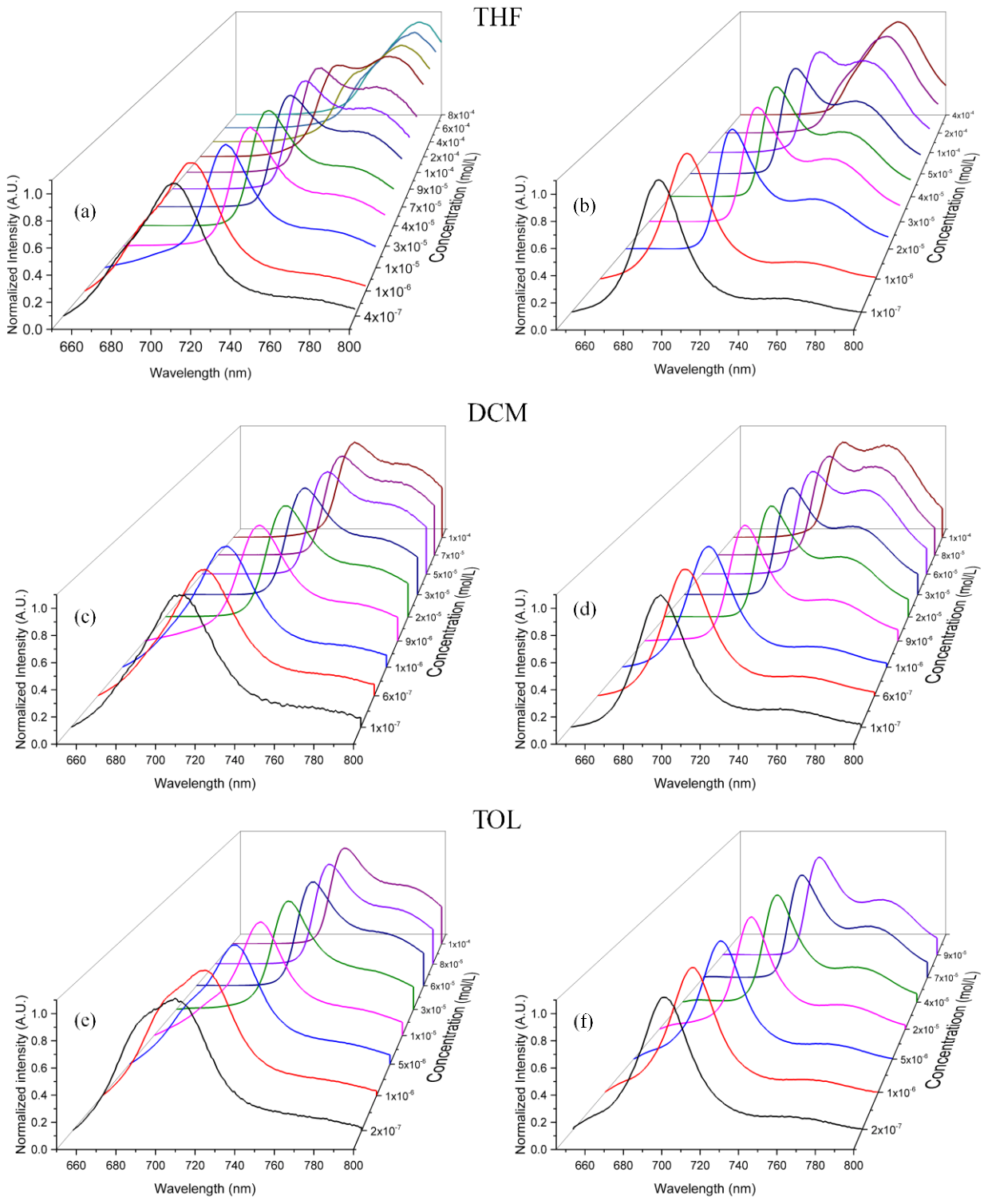

Figure 6: Fluorescence emission spectra of 1 (a, c, e) and 2 (b, d, f) measured at different concentrations in THF, DCM and TOL.

Figure 5 also reveals the appearance of a broad red-shifted fluorescence band as the concentration of the respective dyes were increased due to the formation of excited-state dimers (excimers). The excimer bands were located at c.a. 774 and 754 nm for 1 and 2 respectively. These results suggest that both the excimer formation and reabsorption are playing an important role as can be expected from the overlapping of the absorption as well as from emission spectra and the small stokes shift.

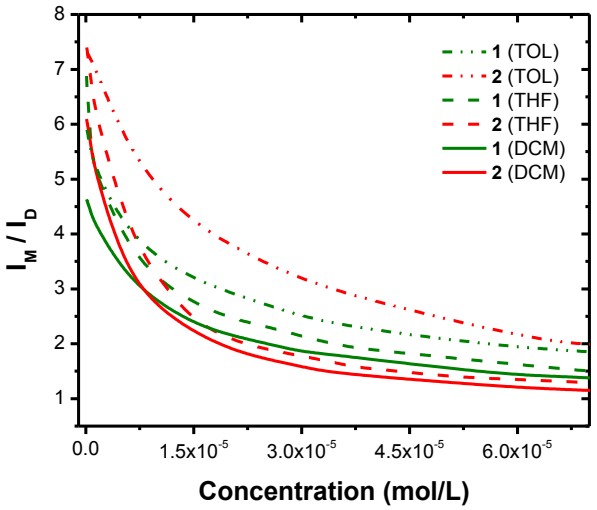

Figure 7: Plot of I_M/I_D of 1 (green line) and 2 (red line) recorded in TOL, THF and DCM at different concentrations.

The data shown indicates that for these molecules the excimer signals do not reach intensities comparable to the monomer emission band at the concentration range in study. This result can be attributed to either a low excimer quantum efficiency, or to strong repulsive intermolecular interactions[6, 15, 17, 60] Moreover, it can be discerned from Figure 5 that in DCM and THF the excimer emission becomes as intense as the monomer signal at concentrations reaching 5×10^{-5} M however this was not the case when using TOL as the solvent. A comparison of the monomer (I_M) to excimer (I_D) intensity ratio for the compounds in the three solvents is shown in

Figure 6 for both dyes. In general the I_M/I_D ratio was higher in TOL followed by THF and finally DCM, this trend is in correspondence with the viscosity of the solvents used, which is in agreement with the fact that the excimer formation is a diffusion controlled process as it involves the transport of the molecules through the solvent media.[14-15] Moreover, the normalized absorption spectra of both dyes in THF showed no significant change in the concentration range. This result, added to the viscosity dependence allowed us to assume that the dynamic excimer (D*) formation:

$$A + h\nu \rightarrow A^*$$

$$A^* + A \rightarrow D^*$$

prevailed over the excitation of preassociated dimers (static excimer).[13] Overall, it can be expected that this new approach would lead to low excimer signals which is desired for optoelectronic applications.

3.5 Quantum Chemical Calculations

The resulting optimized structures (Figure 7) for the compounds from the quantum chemical calculations show a planar vinyl-tetramethylindolium-flanked squaraine core, though in the case of 1 this planarity does not extend out to the pyrene moieties (Figure 7a), as they lay twisted by ~25 °. This distortion appears to have little impact on the conjugation of the molecule however, as the frontier molecular orbitals of the two compounds are equally distributed across the chromophores (Figure 8).

The structures of both optimized dyes allow us to corroborate that the slightly higher photostability of 2 is due to the greater conjugation through all the π-system, and also that the aggregation in this compound is easier than in case of compound 1.

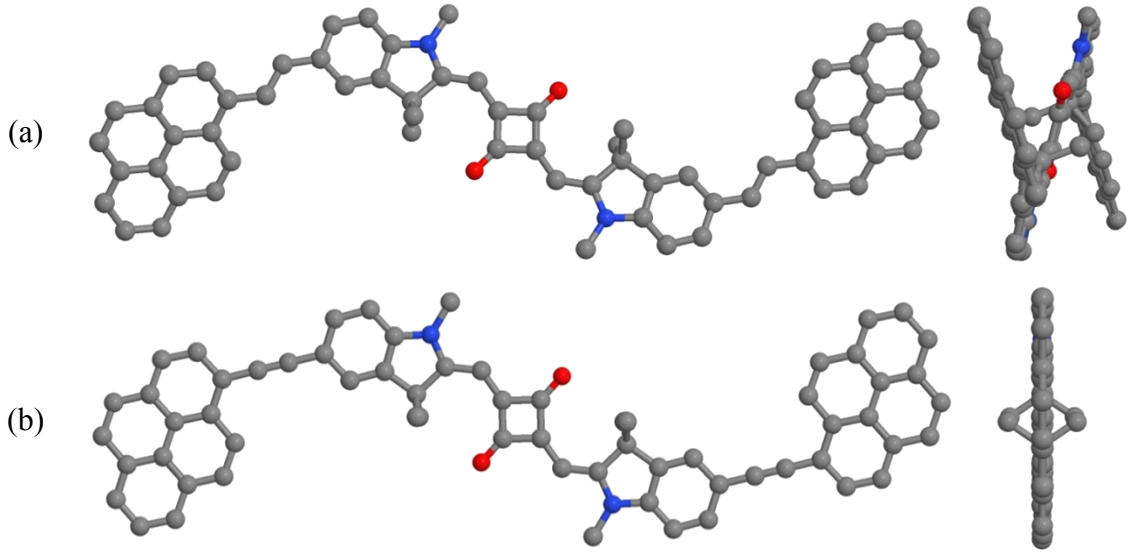

Figure 8: Optimized structure of 1 (a) and 2 (b), front (left) and side view (right).

In the case of both compounds, the electron density in the HOMO and LUMO is centered on the squaraine core; the overlap between the two states leads to the narrow absorption profile. The opposing symmetries of these HOMO and LUMO states make single photon excitation possible; however since two-photon excitation utilizes an intermediary virtual state, this process requires states with like symmetry, resulting in the majority of nonlinear excitation to shorter wavelengths.

The TD-DFT results (Tables 2 and 3) can be used to generate calculated absorption spectra (Figure 9). The first calculated transition at ≈ 630-645 nm is slightly blue-shifted from the experimental absorption maxima, but in both cases represent a single transition: HOMO - LUMO. At shorter wavelength (≈ 400-410 nm), a higher energy transition is seen primarily between HOMO-1 and LUMO+1 overlaps with the short wavelength band seen experimentally, and assigned to the pyrene moieties.

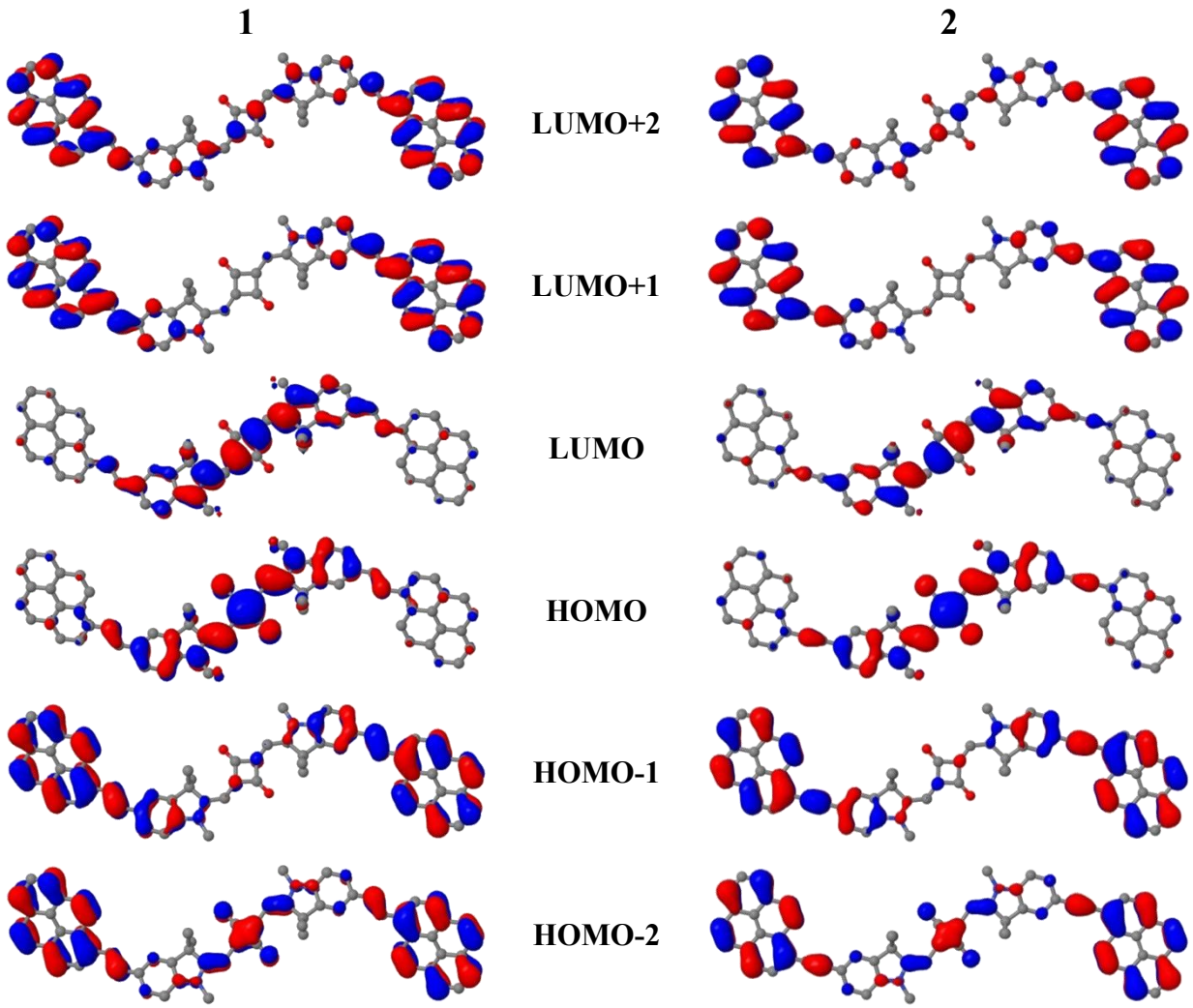

Figure 9: Frontier molecular orbitals for 1 (left) and 2 (right).

Table 2: Calculated properties of the 15 lowest singlet excited states for 1 determined through TD-DFT.[a]

Transition number	Energy /eV	Wavelength /nm	Oscillator strength	Leading configuration	
1	1.93	644	2.49	H → L	0.95
2	2.31	537	0.00	H-3 → L	0.96
3	2.34	530	0.00	H-1 → L	0.75
4	2.45	507	0.01	H-2 → L H → L+2	0.61 0.37
5	2.48	501	0.00	H → L+1	0.75
6	2.65	468	0.18	H-2 → L	0.34

Transition number	Energy /eV	Wavelength /nm	Oscillator strength	Leading configuration	
				H → L+2	0.58
7	3.05	407	0.98	H-1 → L+1	0.89
8	3.08	402	0.00	H-4 → L H-1 → L+2	0.25 0.59
9	3.13	396	0.00	H-4 → L H → L+3	0.39 0.26
10	3.14	394	0.00	H-2 → L+1	0.71
11	3.19	389	0.02	H-5 → L H → L+4	0.65 0.21
12	3.23	384	0.33	H-2 → L+2	0.81
13	3.26	380	0.00	H-8 → L	0.96
14	3.32	373	0.00	H-4 → L H → L+3	0.29 0.50
15	3.33	373	0.06	H-5 → L H → L+4	0.26 0.47

[a] H = HOMO, L = LUMO

Table 3: Calculated properties of the 15 lowest singlet excited states for 2 determined through TD-DFT.[a]

Transition number	Energy /eV	Wavelength /nm	Oscillator strength	Leading configuration	
1	1.96	633	2.51	H → L	0.95
2	2.29	541	0.00	H-3 → L	0.97
3	2.39	520	0.00	H-1 → L	0.74
4	2.48	499	0.01	H-2 → L H → L+2	0.59 0.40
5	2.50	495	0.00	H → L+1	0.75
6	2.67	465	0.18	H-2 → L H → L+2	0.37 0.56
7	3.09	401	0.90	H-1 → L+1	0.88
8	3.12	397	0.00	H-1 → L+2	0.64
9	3.19	389	0.00	H-2 → L+1	0.57
10	3.23	384	0.00	H-4 → L H → L+3	0.45 0.22
11	3.25	382	0.14	H-5 → L H-2 → L+2	0.47 0.40
12	3.25	382	0.00	H-8 → L	0.97
13	3.28	378	0.21	H-5 → L H-2 → L+2	0.29 0.51
14	3.40	364	0.06	H-5 → L	0.11

Transition number	Energy /eV	Wavelength /nm	Oscillator strength	Leading configuration	
				H → L+4	0.47
15	3.41	364	0.00	H-4 → L H → L+3	0.19 0.48

[a] H = HOMO, L = LUMO

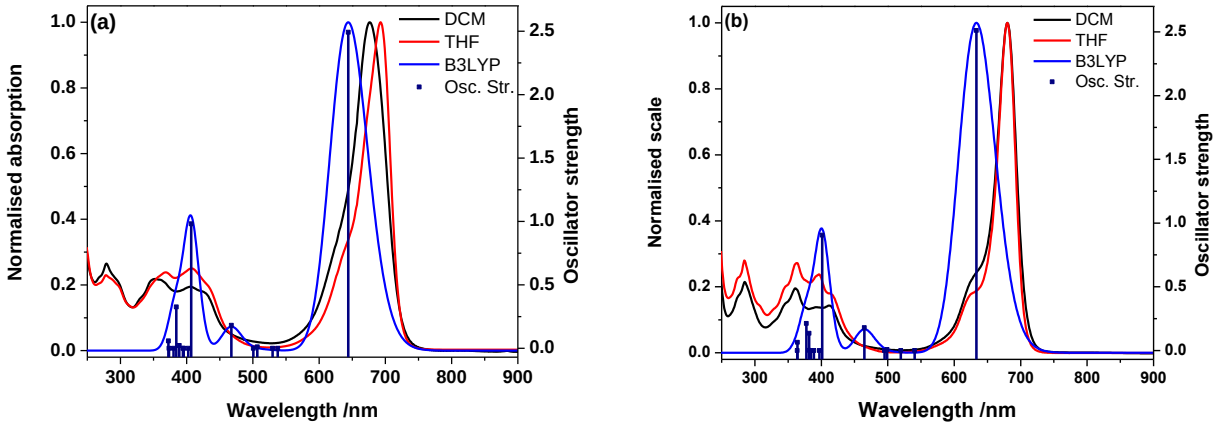

Figure 10: Calculated absorption spectra (blue) and oscillator strengths (dark blue bars) for 1 (a) and 2 (b) overlaid on the respective absorption spectra in DCM (black) and THF (red).

CHAPTER 4: CONCLUSIONS

Two bis(pyrene)-substituted squaraine dyes were synthesized using vinyl and ethynyl bridges and their linear and nonlinear photophysical properties have been characterized using solvents of different polarity. Both dyes presented high photochemical stability, large extinction coefficients as well as high fluorescence quantum yields. Moreover, both derivatives showed a relatively broad two-photon absorption with $\delta > 400$ GM over different spectral regions and with maxima in the two-photon absorption spectra exceeding 10,000 GM. The 2PA spectra of both dyes synthesized in this work revealed an improved charge transfer interaction compared with the indole based squaraine dye, due to the extended conjugated π- system.[39, 61-62] There were some differences in 2PA behavior observed between the two derivatives, but these differences were relatively small. Excimer formation was observed even at room temperature. However, the magnitude of the excimer signal was affected due to the absorption of the fluorescence emission as both derivatives possess very small Stokes shifts.

These results suggest that the inclusion of electron donor-acceptor-donor interaction in pyrene-based derivatives could be a good approach in the design of materials containing PAHs with bright red, green and blue (RGB) emission in the development of full-color displays. This new approach involves the inclusion of an electron acceptor group interconnecting both pyrene moieties. Future studies include the spectroscopic characterization of these compounds in the solid phase as part of the search for improved materials with enhanced optoelectronic properties.

APPENDIX:
^{1}H AND ^{13}C NMR SPECTRA OF NEW COMPOUNDS

^{1}H-NMR of Compound 7

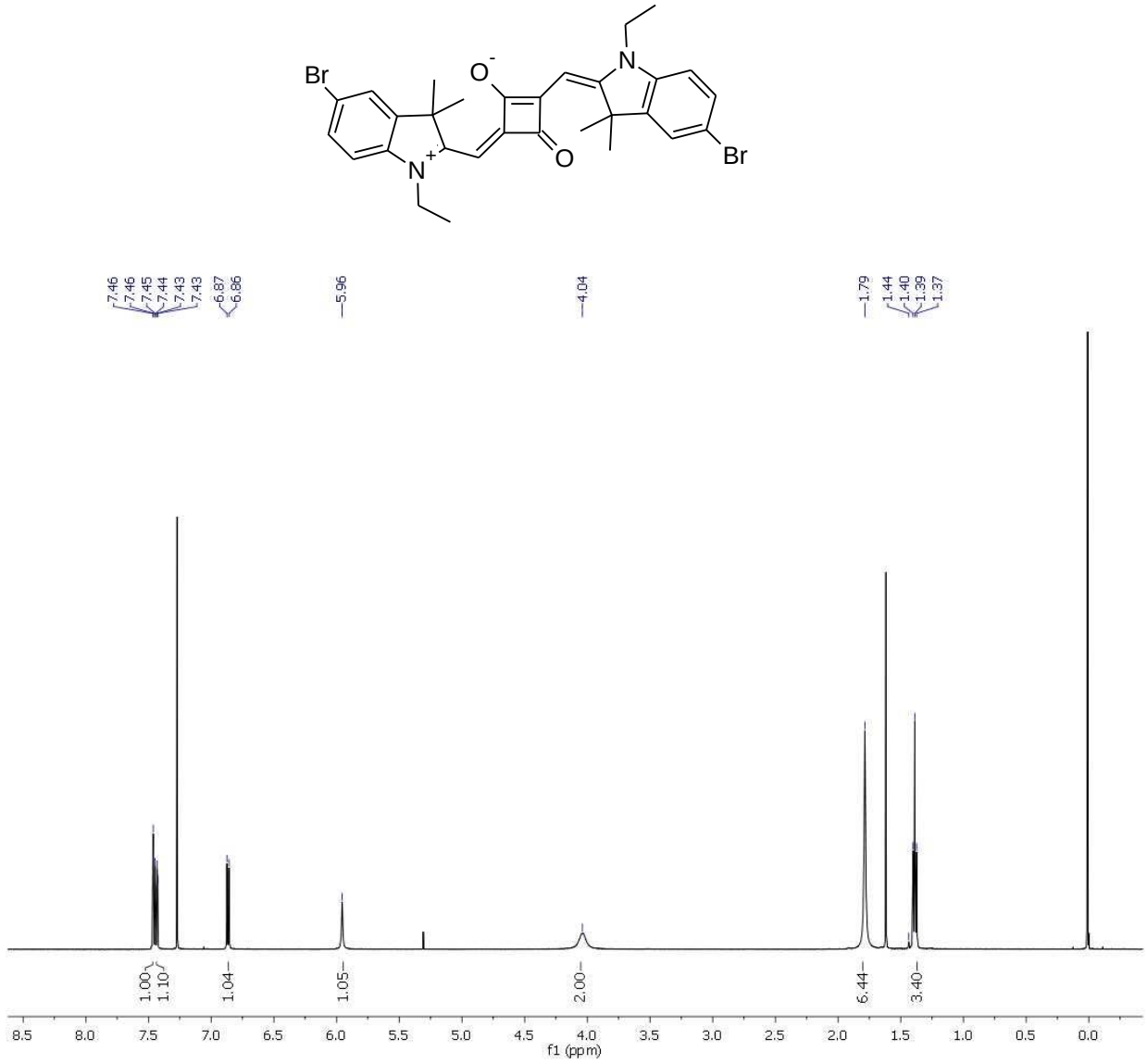

^{13}C-NMR of Compound 7

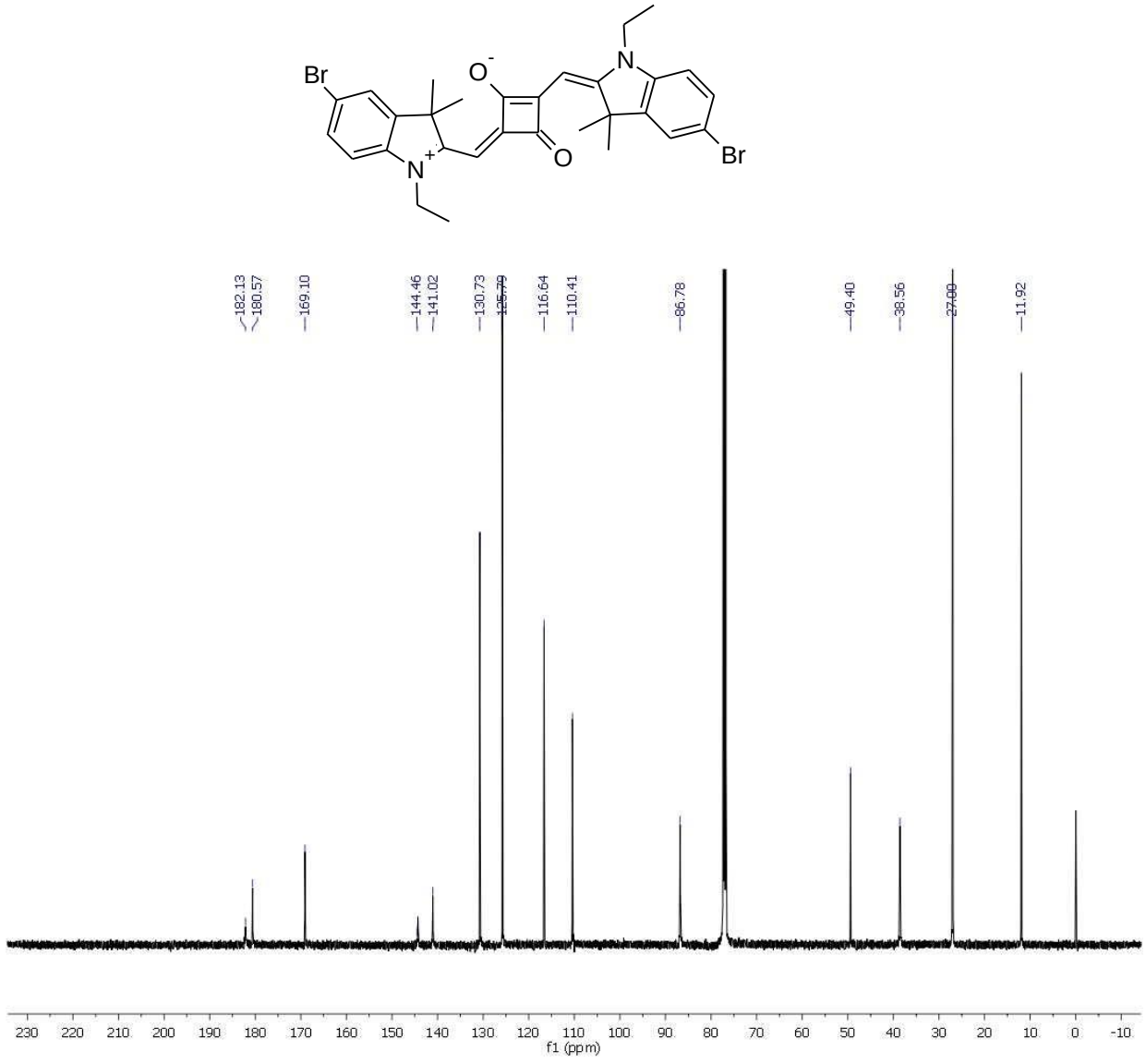

^{1}H-NMR of 1

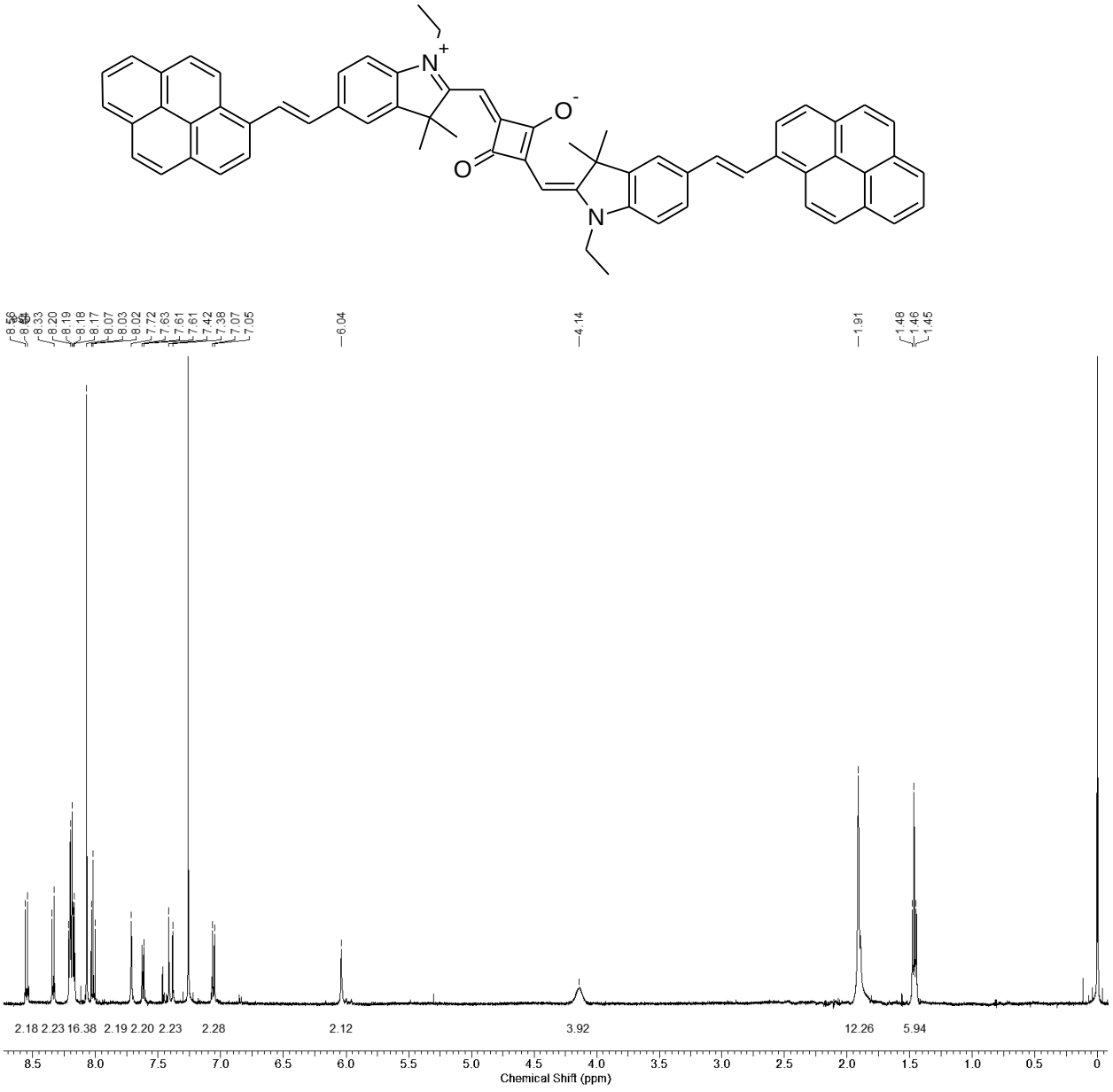
8.56
8.54
8.33
8.20
8.19
8.18
8.17
8.07
8.03
8.02
7.72
7.63
7.61
7.61
7.42
7.38
7.07
7.05
6.04
4.14
1.91
1.48
1.46
1.45
2.18 2.23 16.38 2.19 2.20 2.23 2.28 2.12 3.92 12.26 5.94
Chemical Shift (ppm)

^{13}C-NMR of 1

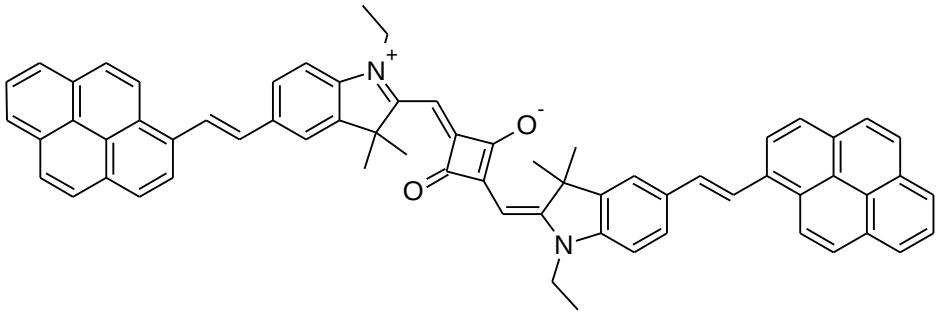
N+
O-
O
N

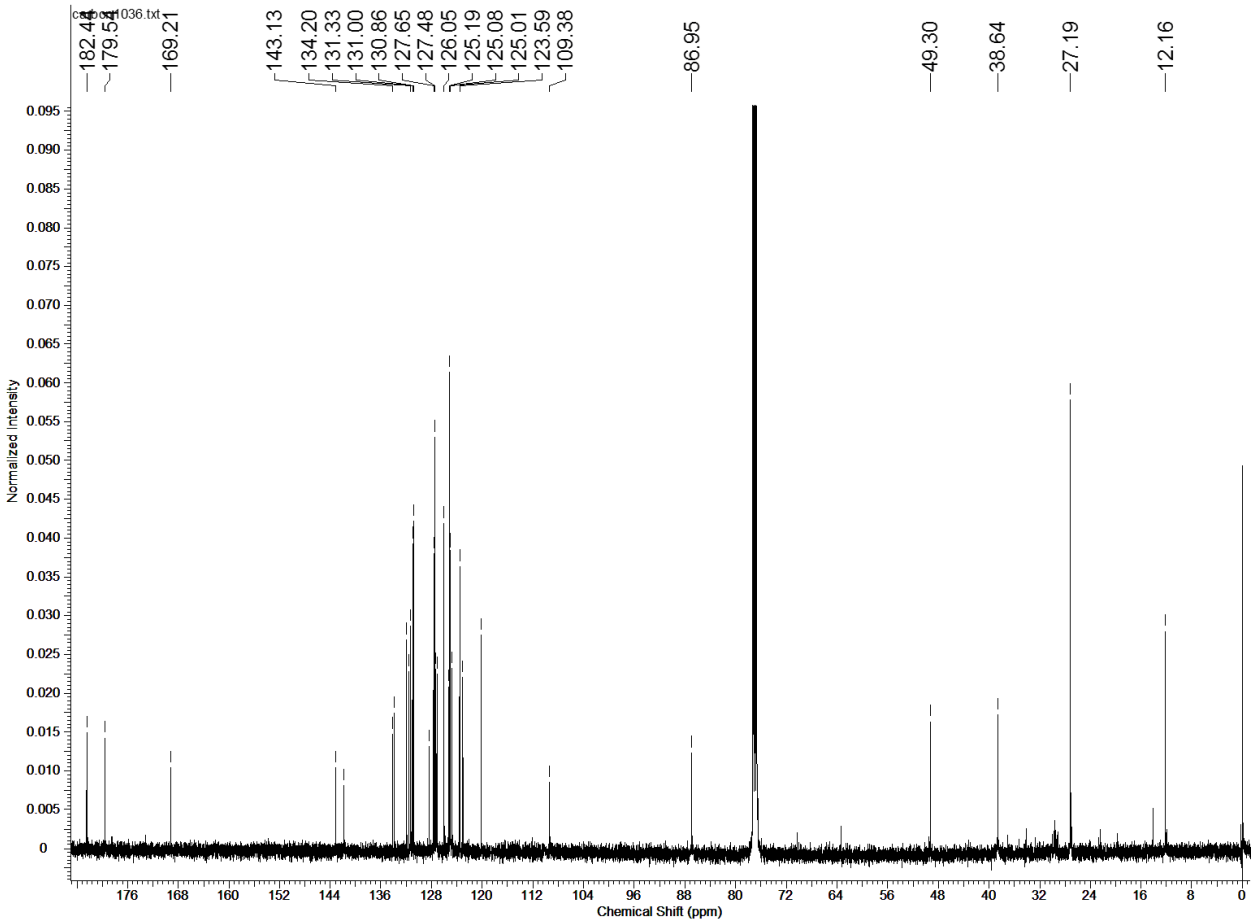
182.44
179.54
169.21
143.13
134.20
131.33
131.00
130.86
127.65
127.48
126.05
125.19
125.08
125.01
123.59
109.38
86.95
49.30
38.64
27.19
12.16
Normalized Intensity
Chemical Shift (ppm)

^{1}H-NMR of 2

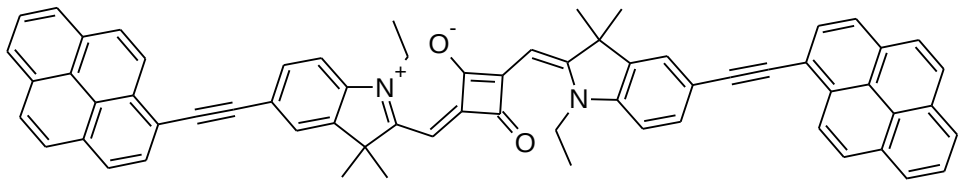

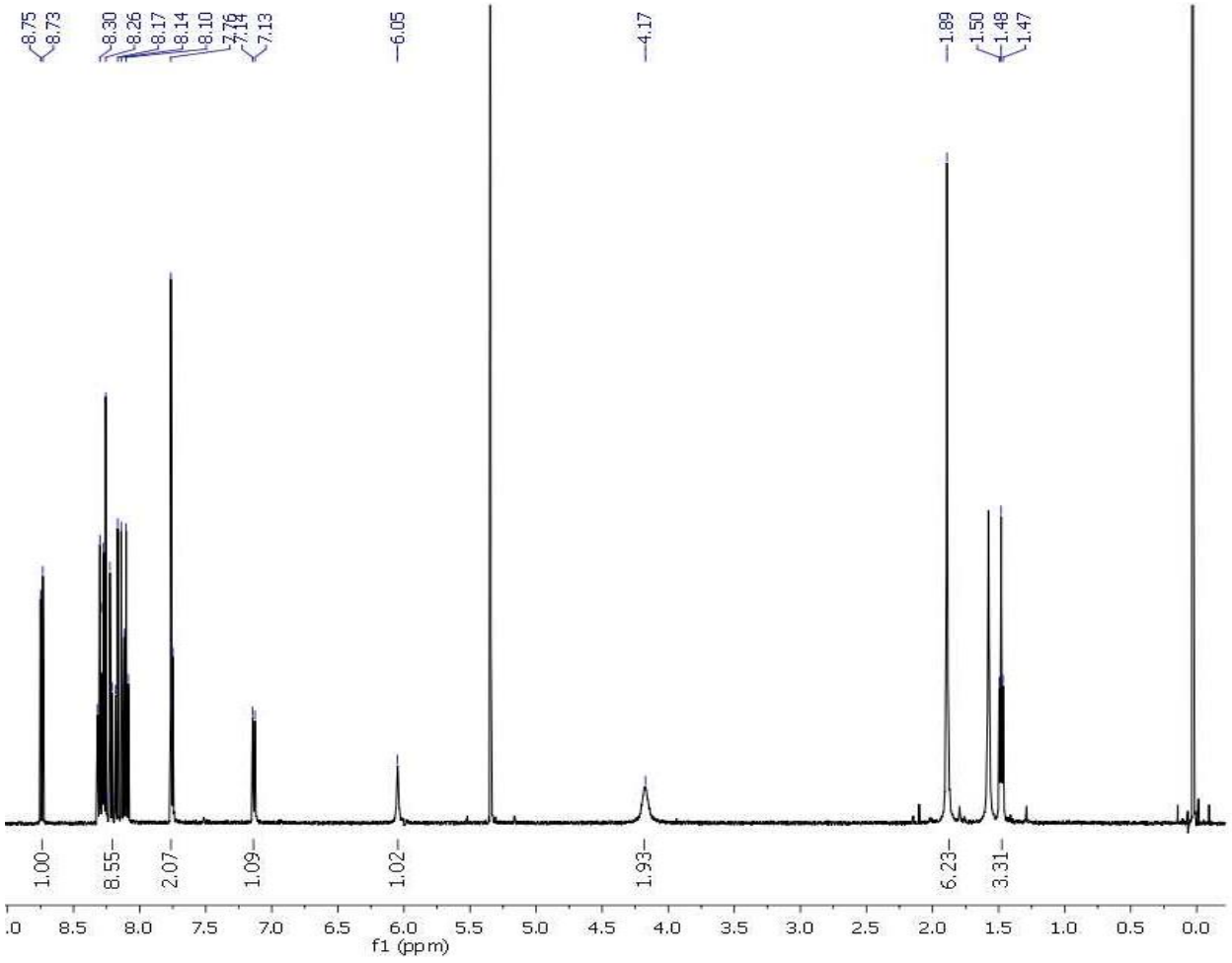
8.75
8.73
8.30
8.26
8.17
8.14
8.10
7.76
7.14
7.13
6.05
4.17
1.89
1.50
1.48
1.47
1.00
8.55
2.07
1.09
1.02
1.93
6.23
3.31
f1 (ppm)

^{13}C-NMR of 2

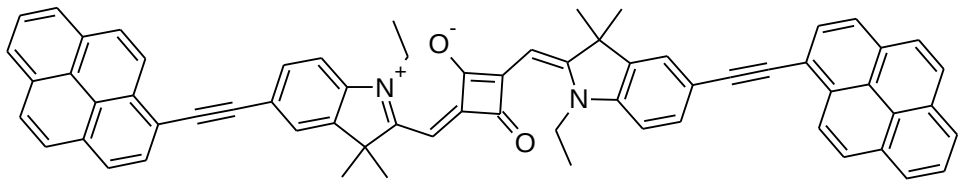
O
-
N
+
O
N

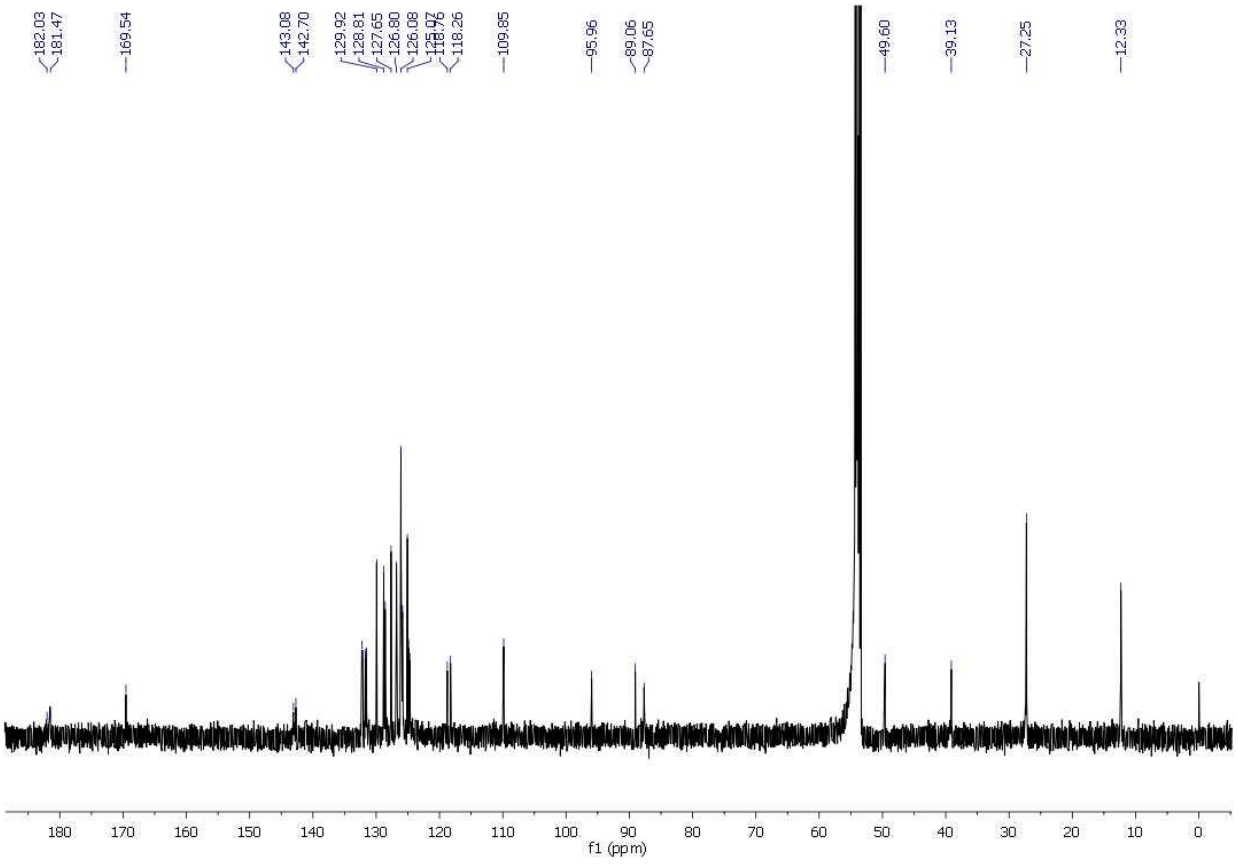
182.03
181.47
169.54
143.08
142.70
129.92
128.81
127.65
126.80
126.08
118.26
109.85
95.96
89.06
87.65
49.60
39.13
27.25
12.33
180
170
160
150
140
130
120
110
100
90
80
70
60
50
40
30
20
10
0
f1 (ppm)

LIST OF REFERENCES

1. Tang, C. W.; VanSlyke, S. A., Organic Electroluminescent Diodes. *Appl. Phys. Lett.* **1987**, *51*, 913-915.

2. Chercka, D.; Yoo, S.-J.; Baumgarten, M.; Kim, J.-J.; Mullen, K., Pyrene Based Materials for Exceptionally Deep Blue Oleds. *J. Mater. Chem. C* **2014**, *2*, 9083-9086.

3. Figueira-Duarte, T. M.; Müllen, K., Pyrene-Based Materials for Organic Electronics. *Chem. Rev.* **2011**, *111*, 7260-7314.

4. Suzuki, K.; Seno, A.; Tanabe, H.; Ueno, K., New Host Materials for Blue Emitters. *Synth. Met.* **2004**, *143*, 89-96.

5. Yang, C.-H.; Guo, T.-F.; Sun, I. W., Highly Efficient Greenish Blue-Emitting Organic Diodes Based on Pyrene Derivatives. *J. Lumin.* **2007**, *124*, 93-98.

6. Birks, J. B., *Photophysics of Aromatic Molecules*; Wiley-Interscience: London, 1970.

7. Hu, J.-Y.; Yamato, T., *Synthesis and Photophysical Properties of Pyrene-Based Light-Emitting Monomers: Highly Blue Fluorescent Multiply-Conjugated-Shaped Architectures*; InTech, 2011.

8. Wu, K. C.; Ku, P. J.; Lin, C. S.; Shih, H. T.; Wu, F. I.; Huang, M. J.; Lin, J. J.; Chen, I. C.; Cheng, C. H., The Photophysical Properties of Dipyrenylbenzenes and Their Application as Exceedingly Efficient Blue Emitters for Electroluminescent Devices. *Adv. Funct. Mater.* **2008**, *18*, 67-75.

9. Cho, H.; Lee, S.; Cho, N. S.; Jabbour, G. E.; Kwak, J.; Hwang, D.-H.; Lee, C., High-Mobility Pyrene-Based Semiconductor for Organic Thin-Film Transistors. *ACS Applied Materials & Interfaces* **2013**, *5*, 3855-3860.

10. Kwon, J.; Hong, J.-P.; Noh, S.; Kim, T.-M.; Kim, J.-J.; Lee, C.; Lee, S.; Hong, J.-I., Pyrene End-Capped Oligothiophene Derivatives for Organic Thin-Film Transistors and Organic Solar Cells. *New J. Chem.* **2012**, *36*, 1813-1818.

11. Zophel, L.; Beckmann, D.; Enkelmann, V.; Chercka, D.; Rieger, R.; Mullen, K., Asymmetric Pyrene Derivatives for Organic Field-Effect Transistors. *Chem. Commun.* **2011**, *47*, 6960-6962.

12. Yamana, K.; Iwai, T.; Ohtani, Y.; Sato, S.; Nakamura, M.; Nakano, H., Bis-Pyrene-Labeled Oligonucleotides: Sequence Specificity of Excimer and Monomer Fluorescence Changes Upon Hybridization with DNA. *Bioconjugate Chem.* **2002**, *13*, 1266-1273.

13. Winnik, F. M., Photophysics of Preassociated Pyrenes in Aqueous Polymer Solutions and in Other Organized Media. *Chem. Rev.* **1993**, *93*, 587-614.

14. Birks, J. B.; Dyson, D. J.; Munro, I. H., 'Excimer'; Fluorescence. Ii. Lifetime Studies of Pyrene Solutions. *Proc. Roy. Soc. London, Ser A Mat.* **1963**, *275*, 575-588.

15. Bowen, E. J., The Photochemistry of Aromatic Hydrocarbon Solutions. In *Advances in Photochemistry*, John Wiley & Sons, Inc.: 1963; pp 23-42.

16. Mikroyannidis, J. A.; Fenenko, L.; Adachi, C., Synthesis and Photophysical Characteristics of 2,7-Fluorenevinylene-Based Trimers and Their Electroluminescence. *J. Phys. Chem. B* **2006**, *110*, 20317-20326.

17. Stevens, B., Photoassociation in Aromatic Systems. In *Advances in Photochemistry*, John Wiley & Sons, Inc.: 1971; pp 161-226.

18. Zhao, K.; Liu, T.; Wang, G.; Chang, X.; Xue, D.; Belfield, K. D.; Fang, Y., A Butterfly-Shaped Pyrene Derivative of Cholesterol and Its Uses as a Fluorescent Probe. *J. Phys. Chem. B* **2013**, *117*, 5659-5667.

19. Strickler, J. H.; Webb, W. W., Three-Dimensional Optical Data Storage in Refractive Media Bytwo-Photon Point Excitation. *Opt. Lett.* **1991**, *16*, 1780-1782.

20. Frederiksen, P. K.; McIlroy, S. P.; Nielsen, C. B.; Nikolajsen, L.; Skovsen, E.; Jørgensen, M.; Mikkelsen, K. V.; Ogilby, P. R., Two-Photon Photosensitized Production of Singlet Oxygen in Water. *J. Am. Chem. Soc.* **2005**, *127*, 255-269.

21. Denk, W.; Strickler, J.; Webb, W., Two-Photon Laser Scanning Fluorescence Microscopy. *Science* **1990**, *248*, 73-76.

22. Maruo, S.; Nakamura, O.; Kawata, S., Three-Dimensional Microfabrication with Two-Photon-Absorbed Photopolymerization. *Opt. Lett.* **1997**, *22*, 132-134.

23. Patel, C. K. N.; Fleury, P. A.; Slusher, R. E.; Frisch, H. L., Multiphoton Plasma Production and Stimulated Recombination Radiation in Semiconductors. *Phys. Rev. Lett.* **1966**, *16*, 971-974.

24. Belfield, K. D.; Bondar, M. V.; Haniff, H. S.; Mikhailov, I. A.; Luchita, G.; Przhonska, O. V., Superfluorescent Squaraine with Efficient Two-Photon Absorption and High Photostability. *ChemPhysChem* **2013**, *14*, 3532-3542.

25. Beverina, L.; Salice, P., Squaraine Compounds: Tailored Design and Synthesis Towards a Variety of Material Science Applications. *Eur. J. Org. Chem.* **2010**, *2010*, 1207-1225.

26. Chung, S.-J., et al., Extended Squaraine Dyes with Large Two-Photon Absorption Cross-Sections. *J. Am. Chem. Soc.* **2006**, *128*, 14444-14445.

27. Sreejith, S.; Carol, P.; Chithra, P.; Ajayaghosh, A., Squaraine Dyes: A Mine of Molecular Materials. *Journal of Materials Chemistry* **2008**, *18*, 264-274.

28. Belfield, K. D.; Bondar, M. V.; Morales, A. R.; Frazer, A.; Mikhailov, I. A.; Przhonska, O. V., Photophysical Properties and Ultrafast Excited-State Dynamics of a New Two-Photon Absorbing Thiopyranyl Probe. *J. Phys. Chem. C* **2013**, *117*, 11941-11952.

29. Belfield, K. D.; Bondar, M. V.; Morales, A. R.; Yue, X.; Luchita, G.; Przhonska, O. V.; Kachkovsky, O. D., Two-Photon Absorption and Time-Resolved Stimulated Emission Depletion Spectroscopy of a New Fluorenyl Derivative. *ChemPhysChem* **2012**, *13*, 3481-3491.

30. Corredor, C. C.; Belfield, K. D.; Bondar, M. V.; Przhonska, O. V.; Yao, S., One- and Two-Photon Photochemical Stability of Linear and Branched Fluorene Derivatives. *J. Photochem. Photobiol., A* **2006**, *184*, 105-112.

31. Fu, J.; Padilha, L. A.; Hagan, D. J.; Van Stryland, E. W.; Przhonska, O. V.; Bondar, M. V.; Slominsky, Y. L.; Kachkovski, A. D., Experimental and Theoretical Approaches to Understanding Two-Photon Absorption Spectra in Polymethine and Squaraine Molecules. *J. Opt. Soc. Am. B* **2007**, *24*, 67-76.

32. Fu, J.; Padilha, L. A.; Hagan, D. J.; Van Stryland, E. W.; Przhonska, O. V.; Bondar, M. V.; Slominsky, Y. L.; Kachkovski, A. D., Molecular Structure Two-Photon Absorption Property Relations in Polymethine Dyes. *J. Opt. Soc. Am. B* **2007**, *24*, 56-66.

33. Morales, A. R.; Frazer, A.; Woodward, A. W.; Ahn-White, H.-Y.; Fonari, A.; Tongwa, P.; Timofeeva, T.; Belfield, K. D., Design, Synthesis, and Structural and Spectroscopic Studies of Push–Pull Two-Photon Absorbing Chromophores with Acceptor Groups of Varying Strength. *J. Org. Chem.* **2013**, *78*, 1014-1025.

34. Scherer, D.; Dörfler, R.; Feldner, A.; Vogtmann, T.; Schwoerer, M.; Lawrentz, U.; Grahn, W.; Lambert, C., Two-Photon States in Squaraine Monomers and Oligomers. *Chem. Phys.* **2002**, *279*, 179-207.

35. Webster, S.; Fu, J.; Padilha, L. A.; Przhonska, O. V.; Hagan, D. J.; Van Stryland, E. W.; Bondar, M. V.; Slominsky, Y. L.; Kachkovski, A. D., Comparison of Nonlinear Absorption in Three Similar Dyes: Polymethine, Squaraine and Tetraone. *Chem. Phys.* **2008**, *348*, 143-151.

36. Ajayaghosh, A., Chemistry of Squaraine-Derived Materials: Near-Ir Dyes, Low Band Gap Systems, and Cation Sensors. *Acc. Chem. Res.* **2005**, *38*, 449-459.

37. Bae, S. H.; Seo, K. D.; Choi, W. S.; Hong, J. Y.; Kim, H. K., Near-Ir Organic Sensitizers Containing Squaraine and Phenothiazine Units for Dye-Sensitized Solar Cells. *Dyes Pigments* **2015**, *113*, 18-26.

38. Fang, Y.; Li, Z.; Yang, B.; Xu, S.; Hu, X.; Liu, Q.; Han, D.; Lu, D., Effect of Dye Structure on Optical Properties and Photocatalytic Behaviors of Squaraine-Sensitized Tio2 Nanocomposites. *J. Phys. Chem. C* **2014**, *118*, 16113-16125.

39. Moreshead, W. V.; Przhonska, O. V.; Bondar, M. V.; Kachkovski, A. D.; Nayyar, I. H.; Masunov, A. E.; Woodward, A. W.; Belfield, K. D., Design of a New Optical Material with

Broad Spectrum Linear and Two-Photon Absorption and Solvatochromism. *J. Phys. Chem. C* **2013**, *117*, 23133-23147.

40. Lin, V.; DiMagno, S.; Therien, M., Highly Conjugated, Acetylenyl Bridged Porphyrins: New Models for Light-Harvesting Antenna Systems. *Science* **1994**, *264*, 1105-1111.

41. Lin, V. S. Y.; Therien, M. J., The Role of Porphyrin-to-Porphyrin Linkage Topology in the Extensive Modulation of the Absorptive and Emissive Properties of a Series of Ethynyl- and Butadiynyl-Bridged Bis- and Tris(Porphinato)Zinc Chromophores. *Chem. Eur. J.* **1995**, *1*, 645-651.

42. He, G. S.; Tan, L.-S.; Zheng, Q.; Prasad, P. N., Multiphoton Absorbing Materials: Molecular Designs, Characterizations, and Applications. *Chem. Rev.* **2008**, *108*, 1245-1330.

43. Kim, H. M.; Lee, Y. O.; Lim, C. S.; Kim, J. S.; Cho, B. R., Two-Photon Absorption Properties of Alkynyl-Conjugated Pyrene Derivatives. *J. Org. Chem.* **2008**, *73*, 5127-5130.

44. Kozma, E.; Munno, F.; Kotowski, D.; Bertini, F.; Luzzati, S.; Catellani, M., Synthesis and Characterization of Perylene-Based Donor–Acceptor Copolymers Containing Triple Bonds. *Synth. Met.* **2010**, *160*, 996-1001.

45. Thomas, K. R. J.; Kapoor, N.; Bolisetty, M. N. K. P.; Jou, J.-H.; Chen, Y.-L.; Jou, Y.-C., Pyrene-Fluorene Hybrids Containing Acetylene Linkage as Color-Tunable Emitting Materials for Organic Light-Emitting Diodes. *J. Org. Chem.* **2012**, *77*, 3921-3932.

46. Zang, L.; Che, Y.; Moore, J. S., One-Dimensional Self-Assembly of Planar Π-Conjugated Molecules: Adaptable Building Blocks for Organic Nanodevices. *Acc. Chem. Res.* **2008**, *41*, 1596-1608.

47. Wang, J.; Leung, L. M., Self-Assembly and Aggregation of Atrp Prepared Amphiphilic Bab Tri-Block Copolymers Contained Nonionic Ethylene Glycol and Fluorescent 9,10-Di(1-Naphthalenyl)-2-Vinyl-Anthracene/1-Vinyl-Pyrene Segments. *Eur. Polym. J.* **2013**, *49*, 3722-3733.

48. Lakowicz, J. R., *Principles of Fluorescence Spectroscopy*, 3rd ed.; Kluwer Academic/Plenum Publishers, 2007.

49. Frisch, M. J., et al. *Gaussian 09*, Gaussian, Inc.: Wallingford, CT, USA, 2009.

50. Mongin, O.; Porrès, L.; Charlot, M.; Katan, C.; Blanchard-Desce, M., Synthesis, Fluorescence, and Two-Photon Absorption of a Series of Elongated Rodlike and Banana-Shaped Quadrupolar Fluorophores: A Comprehensive Study of Structure–Property Relationships. *Chem. Eur. J.* **2007**, *13*, 1481-1498.

51. Azim, S. A.; Al-Hazmy, S. M.; Ebeid, E. M.; El-Daly, S. A., A New Coumarin Laser Dye 3-(Benzothiazol-2-Yl)-7-Hydroxycoumarin. *Opt. Laser Technol.* **2005**, *37*, 245-249.

52. Eggeling, C.; Brand, L.; Seidel, C. A. M., Laser-Induced Fluorescence of Coumarin Derivatives in Aqueous Solution: Photochemical Aspects for Single Molecule Detection. *Bioimaging* **1997**, *5*, 105-115.

53. Soper, S. A.; Nutter, H. L.; Keller, R. A.; Davis, L. M.; Shera, E. B., The Photophysical Constants of Several Fluorescent Dyes Pertaining to Ultrasensitive Fluorescence Spectroscopy. *Photochem. Photobiol.* **1993**, *57*, 972-977.

54. Pawlicki, M.; Collins, H. A.; Denning, R. G.; Anderson, H. L., Two-Photon Absorption and the Design of Two-Photon Dyes. *Angew. Chem. Int. Ed.* **2009**, *48*, 3244-3266.

55. Eisfeld, A.; Briggs, J. S., The J- and H-Bands of Organic Dye Aggregates. *Chem. Phys.* **2006**, *324*, 376-384.

56. Sherwood, G. A.; Cheng, R.; Smith, T. M.; Werner, J. H.; Shreve, A. P.; Peteanu, L. A.; Wildeman, J., Aggregation Effects on the Emission Spectra and Dynamics of Model Oligomers of Meh-Ppv. *J. Phys. Chem. C* **2009**, *113*, 18851-18862.

57. Kasha, M.; Rawls, H. R.; El-Bayoumi, A., The Exciton Model in Molecular Spectroscopy. *Pure Appl. Chem.* **1965**, *11*, 371-392.

58. Roden, J.; Eisfeld, A.; Briggs, J. S., The J- and H-Bands of Dye Aggregate Spectra: Analysis of the Coherent Exciton Scattering (Ces) Approximation. *Chem. Phys.* **2008**, *352*, 258-266.

59. Sauer, M.; Hofkens, J.; Enderlein, J., Basic Principles of Fluorescence Spectroscopy. In *Handbook of Fluorescence Spectroscopy and Imaging*, Wiley-VCH Verlag GmbH & Co. KGaA: 2011; pp 1-30.

60. Halpern, A.; McBane, G., *Experimental Physical Chemistry: A Laboratory Textbook*; W. H. Freeman: New York, 2006.

61. Odom, S. A., et al., Synthesis and Two-Photon Spectrum of a Bis(Porphyrin)-Substituted Squaraine. *J. Am. Chem. Soc.* **2009**, *131*, 7510-7511.

62. Webster, S., et al., Linear and Nonlinear Spectroscopy of a Porphyrin−Squaraine−Porphyrin Conjugated System. *J. Phys. Chem. B* **2009**, *113*, 14854-14867.